PROJECT REVIEW

Digital Image Processing (ITE1010)

MEMBERS

AADISH KALA (17BIT0375)

SURYANSH AGARWAL (17BIT0080)

FACULTY

PROF. PRABUKUMAR M

PROJECT TITLE

Classification of Malignant and Benign tumours of Skin Cancer

CONTENTS

Acknowledgement

In performing our assignment, we had to take the help and guideline of some respected persons, who deserve our greatest gratitude. The completion of this assignment gives us much Pleasure. We would like to show our gratitude Mr. Prabukumar M, our DIP Professor of Vellore Institute of Technology for giving us a good guideline for assignment throughout numerous consultations. We would also like to expand our deepest gratitude to all those who have directly and indirectly guided us in writing this assignment.

Many people, especially our classmates and team members itself, have made valuable comment suggestions on this proposal which gave us an inspiration to improve our assignment. We thank all the people for their help directly and indirectly to complete our assignment.

Abstract

Cancer is a dangerous disease in current time. Various types of cancers are spreading for which skin cancer becomes a very common cancer nowadays. Skin cancer can be of two types namely melanoma and benign cancer. The objective of this project is to detect and classify the benign and malign. Benign meaning the normal image, melanoma the cancerous one. And more over compare the various classification algorithms. Detection of skin cancer in earlier stages can be a life saving process. The detection of skin cancer includes four important stages namely Pre-processing, Segmentation, Feature Extraction and Classification. Detection can help in curing the cancer and hence detection plays a very vital role. In this project, pre-processing the first and the foremost part of image processing which helps in noise removal is done by means of the median filter where the output of the median filter, then the output of median filter is fed as an input to the segmentation phase where we apply watershed algorithm is done to separate the foreground and the background. The segmentation helps to identify the region of interest , which is then passed to neural net CNN . CNN trains on the dataset and then we predict images.

INTRODUCTION

Cancer is expanding step by step in this day and age. The majority of the individuals are experiencing malignant growth. The treatment given during those periods are extremely difficult. There are different phases of malignant growth. Identifying malignant growth in prior stages can get an opportunity to fix the illness. Later organizes are troublesome .The treatment for malignant growth is exceptionally difficult. They need to experience a progression of chemotherapy pursued by a medical procedure whenever required and afterward a radiation. Malignant growth can be in any part of the body. There are different kinds of malignant growth to be specific inward organ and outside organ disease, relatively the fix pace of outer disease is more when contrasted with that of the inside disease. The sorts are bosom, mind, colon, lung, uterus, bladder, cervical, skin, kidney, liver pancreatic, thyroid and part more. This report concentrates much on to the skin malignant growth and identifying of skin disease from the pictures underneath picture

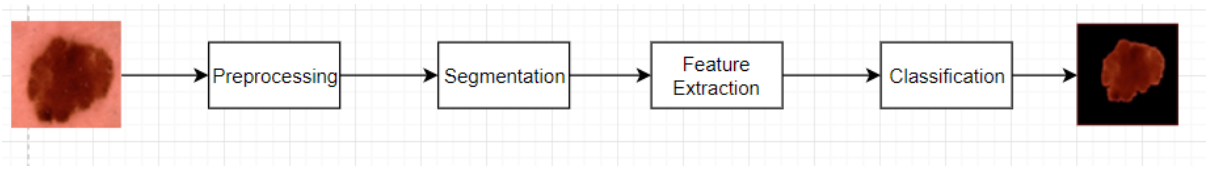

clarifies the different phases of recognition to be specific preprocessing, division, Feature extraction and grouping. There are different sorts of skin malignancy like basal cell carcinoma, squamous cell carcinoma. These are skin tumors that need treatment only high over the minor medications that are being given. The most pivotal thing is at all the sorts of malignant growth it may be there are different stages that includes to be specific stage 1, arrange 2, organize 3 and stage 4. The stage 1 to organize 3 have higher pace of fix, while the stage 4 similarly has a lesser possibility when contrasted with that of different stages. Skin malignancy can have another sort to be specific melanoma, melanoma is

extremely the one which reasons generally the passings. Our point centers around discovering or distinguishing the disease and grouping proportionate to if it is a melanoma or not. Skin harmful developments are caused conventionally to people who open a great deal to the sunshine and besides a melanoma can in like manner be going on the reason on the moles, it can make from the moles. Basal cell carcinoma and squamous cell carcinoma fall under the class of non melanoma threatening development. The proposed system can work as a complete stream from pre-getting ready to the gathering stage as it portrays all of the methods which are locked in with the entire ID of threatening development cells, what's more it furthermore fuses the stages from pre-taking care of to the request which finds the entire movement of the work that will be performed for the area of dangerous domain. The textural features help in extending the exactness of the gathering counts. Furthermore, moreover the relationship of various course of action computation helps in finding which could be a fitting portrayal estimation for the above performed gathering of stages for ID of the melanoma or not. As the proposed method helps in an OK portrayal precision using the assist vector with machining the features considered can be incredible, yet simultaneously this could be improved by using diverse component assurance approach and by thinking about a greater number of features other than an area, mean, standard deviation and contrast. In addition, as a continuation to this the best in class methodology can join dynamically number of features to improve the request rate further.

Related Work & Literarure Survey

The paper [1] portrays on the grouping system of k-law Fourier non straight method. It is accomplished for Red, Blue Green channels where green band is picked. Parallel cover is utilized to duplicate, Fourier change is applied to the outcome, if positive take those qualities else print zero. The pre-preparing technique is done in a recurrence area. Ref. [2] talks on different pre handling strategies improvement, reclamation and hair expulsion techniques. Upgrade manages scaling, differentiate extending and reclamation centers around expelling commotion and evacuating the haze and the hair expulsion incorporates morphological techniques. Ref. [3] proposes on order utilizing back engendering calculation. It characterizes the cells utilizing melanoma and non melanoma. Grouping precision is 100% in the work. Ref. [4] focuses on picture in recurrence area, and is on Fourier ghastly examination. The primary spotlight is on the Fourier examination. Ref. [5] proposes a neural system process notwithstanding fluffy induction framework. The highlights picked here are region and shading and a fundamental neural system is applied for characterization. Ref. [6] preprocessing here is finished by KL change histogram balance, Region of enthusiasm for division utilizing thresholding and factual area merging(SRM) out of which SRM is relatively better dependent on the outcomes referenced, Feature extraction underpins wavelet disintegration and grouping clarifies feed forward system. Ref. [7] clarifies wavelet change for preprocessing and furthermore ABCD [8-10] and fluffy surmising for include extraction and grouping of picture shading seriousness. The proposed technique has the benefit of improving the grouping rate. The highlights removed improve the characterization exactness The calculations picked so far in the proposed technique are moderately better. Also, the arrangement calculations that are utilized are contrasted with give an exactness rate.

Author	Techniques	Dataset	Matrix	Result
Toshiyuki Tanaka, Toinoo Joke, Teruaki Oka2	Segmentation, skin tumor, cell nucleus, dynamic threshold, Laplacian histogram	MRI Scan	20 dermatofibroma and 20 dermatofibrosarcoma with magnification of 40 were used for this research.	Frequency distributions have similar shapes each other, but cumulative frequencies are completely different. This result is the reason that average number of nuclei per one image for dermatofibrosarcoma is much more than that for dermatofibroma.
Zhao Zhang*, William V. Stoecker, and Randy H. Moss	Border detection, radial search, skin tumor	Normal image	A border error less than or equal to 50% is considered acceptable for this research, so 83% of the automatically detected borders are acceptable to human observers.	For the 66-image database, all tumors were found by the center marker. For the larger 299-image test set, only 69% accuracy in tumor finding was noted. Images of this degree of difficulty are best processed by manual border determination by the physician.
Scott E Umbaugh, Randy H. Moss, and William V. Stoecker	IMAGE SEGMENTATION, Clustering Techniques	MRI Scan	73 percent were correctly identified with variegated coloring being present/absent.	These results demonstrated the success of image segmentation by color using a spherical coordinate transform of rectangular RGB space.

Fikret Ercal, Senior Member, IEEE Anurag Chawla, William V. Stoecker,	ARTIFICIAL NEURAL NETWORKS As PATTERN CLASSIFIE	Normal images	80% correct classification of the malignant and benign tumors on real skin tumor images.	or the 60% training percentage, a maximum success rate of 95.8% was obtained for melanomas, while the mean success rate was close to 80%. Mean success rate for correct negative diagnosis (nonmelanoma) was 86.3%. When all the four categories were considered, mean success rate approached 83%.
William Aiaya V.Stoec er2J,4 John P. Cookson5 Scott E. Umbough6 Randy H. Moss	Neural Network Models	Normal images	Often including tan, brown, and red, and sometimes shades of pink and blue. Variegated coloring is believed to be one of the most predictive features for malignant melanoma	A peak accuracy was not very impressive for 80% images.
Lei Bi, Student Member, IEEE, Jinman Kim∗	Dermoscopic, fully convolutional networks (FCN), melanoma, segmentation.	Normal images	ExB was 0.34% lower and CUMED was 1.74% lower while in Table II, ExB was 0.21% higher and CUMED was 1.39% lower to our method in Jaccard measure.	We achieved an average Dice coefficient of 91.18% on the ISBI 2016 Skin Lesion Challenge dataset and 90.66% on the PH2 dataset. Conclusion and Significance: Our extensive experimental results on two well-established public benchmark datasets
Sigurdur Sigurdsson*, Peter Alshede Philipsen, Lars Kai Hansen,	Neural network classifier, neural network visualization, pattern recognition, skin cancer detection.	Normal images	for the present data set, involving 222 cases and five lesion types, was 80.5% 5.3% correct classification of malignant melanoma, which is similar to that of trained dermatologists based on visual inspection.	The skin cancer basal cell carcinoma has a classification rate of 95.8% 2.7%, which is excellent. The overall classification rate of skin lesions is 94.8% 3.0%.
Yading Yuan, Ming Chao, and Yeh-Chi Lo	Deep learning, fully convolutional neural networks, image segmentation, jaccard distance, melanoma, dermoscopy.	Normal images	Five out of these six models achieved performance that place them as the second rank in the 2016 ISBI challenge	Experimental results showed that the proposed method outperformed other state-of-the-art algorithms on these two databases

			on melanoma lesion segmentation, with FCN-6 performing best to yield a Jaccard index of 0.836.	
M. Emre Celebi Noel Codella, and Allan Halpern	Skin cancer, melanoma, dermoscopy, computer-aided diagnosis, dermoscopy image analysis.	Images		
F. Ercal, M. Moganti, W. V. Stoecker, and R. H. Moss	the borders of tumors as an initial step towards the diagnosis of skin tumors from their color images	Images		By experimentation, we found that control points that are 10 points apart resulted in an acceptable smoothing operation that preserved all the crucial elements at the border for the computation of the irregularity index, I, while removing the extra jaggedness originating from the digitization process.
H. S. Ganzeli, J. G. Bottesini, L. O. Paz and M. F. S. Ribeiro	Image recognition, image processing, adaptivity, adaptive devices, dermatology, oncology, skin cancer, software engineering, artificial intelligence.	Images		Table I illustrates the final results with 20 images of 10 melanomas and 10 non-melanomas. O training was performed considering the same amount 210 IEEE LATIN AMERICA TRANSACTIONS, VOL. 9, NO. 2, APRIL 2011 of images and avoiding a sample database addicted.
Maryam Sadeghi, Member, IEEE, Tim K. Lee	Computer-aided diagnosis, dermoscopic structures, dermoscopy, graph, irregular streaks, melanoma, skin cancer, streak detection, texture analysis.	Images	Furthermore, symmetric streaks (starburst pattern) are one of the specific dermoscopic criteria to differentiate usually benign Spitz nevi (a dark nevus common in children) from melanoma, thus increasing diagnostic accuracy for pigmented Spitz nevi from 56% to 93%	Results show Precision, Recall, F-Measure, Accuracy, and AUC of 0.85, 0.87, 0.86, 0.85, and 0.905 for [14] compared with 0.893, 0.893, 0.893, 0.893, and 0.932 for the current work, respectively.

Ilias Maglogiannis, Member, IEEE, and Charalampos N. Doukas,	Classification methods, computer vision, dermoscopy, melanoma, pattern analysis, skin cancer.	Images	accuracy rates from 68.94 (Kstar) to 76.08 (SVM), whereas TPRs from 0 (LWL) to 0.449 (Bayes networks), respectively.	Accuracy ranges from 68.70% (Bayes networks) to 77.06 (SVM), whereas TP from 0.246 (Kstar) to 1.0 (SVM).
M. Emin Yuksel , Senior Member, IEEE, and Murat Borlu	Fuzzy logic, image processing, image thresholding, type-2 fuzzy logic.	Images		As an additional but a subjective evaluation, nevus borders determined by the three methods have been visually evaluated by an expert dermatologist, and the presented type-2 fuzzy-logic-based segmentation method has been found to be superior over the Otsu and the adaptive thresholding methods.
Arve Kjoelen, Scott E. Umbaugh, and MarkZuke	Transform-Domain Coding	Images		Depicts the image 1268n.ppm, which has high correlation coefficients, ranging from 0.995 to 0.998.
Hening Wang, Xin Xu, Xiaoqin Li, Peng Xi, and Qiushi Ren	Imaging Design	Images		observation of the pigment distribution is seriously compromised due to the strong direct reflection of light from the stratum corneum.
F. E. S. Alencar, D. C. Lopes and F. M. Mendes Neto	Image Classification, melanoma, Mobile Devices, Artificial Intelligence, MLP Network, Dermoscopic Images.	Images	According to the results, the system achieved a level of 66% sensitivity and 93% specificity.	Com relação a borda, a presença de ruídos em algumas imagens dificultou a análise das irregularidades de algumas lesões, mas mesmo assim o método ainda obteve um bom resultado, pois o mesmo foi capaz de identificar irregularidades em 88,5% das imagens. Quanto à validação, é necessário apresentar os resultados a um especialista para que o mesmo possa validar a técnica desenvolvida
Lequan Yu,∗ Student Member, IEEE, Hao Chen,	Automated melanoma recognition, fully convolutionalneural networks,residuallearning, skin lesion analysis, very deep convolutional neural networks.	Images	We rank the first place in the challenge with the AP value 0.637, demonstrating the advantages of the proposed method in dealing with the	among 25 teams and 28 teams, respectively. This study corroborates that very deep CNNs with effective training mechanisms can be employed to solve complicated medical image analysis tasks, even with limited training data.

			challenges of the skin lesion recognition	
Costantino Grana, Giovanni Pellacani, Rita Cucchiara, and Stefania Seidenari*	Border, Catmull–Rom splines, epiluminescence, image analysis, melanoma, skin tumor.	Images		The efficacy of these new descriptors was tested on a data set of 510 pigmented skin lesions, composed by 85 melanomas and 425 nevi, by employing statistical methods for discrimination between the two populations.
Huiyu Zhou, Gerald Schaefer, Member, IEEE	Dermoscopy, fuzzy c-means, image segmentation, mean shift, melanoma, skin cancer	Images	The results are presented in Table II from which it can be seen that the proposed AMSFCM takes computation efforts of 37%, 4%, and 17% less than compared to FCM, RSFCM and EnFCM respectively.	Experimental results on a large dataset of diverse dermoscopy images demonstrate that the presented method accurately and efficiently detects the borders of skin lesions.
Ibn Rushd College for Management Science, Abha, Saudi Arabia	Convolutional neural network, skin lesion, novel regularizer, AUC-ROC.	Images	The area under the curve (AUC) achieved for nevus against melanoma lesion, seborrheic keratosis versus basal cell carcinoma lesion, seborrheic keratosis versus melanoma lesion, solar lentigo versus melanoma lesion is 0.77, 0.93, 0.85, and 0.86, respectively.	Our results showed that the proposed learning model outperformed the existing algorithm and can be used to assist medical practitioners in classifying various skin lesions.
Ivan Gonz´ alez-D´ ´ıaz	Skin lesion analysis, melanoma, convolutional neural networks, dermoscopy, CAD.	Images	Furthermore, our results in Specificity at a 95% Sensitivity are clearly better than those of the rest of the approaches, which makes our system very suitable as an automatic filtering module reducing the workload of dermatologists	Our results prove that the incorporation of these subsystems not only improves the performance, but also enhances the diagnosis by providing more interpretable outputs.

LITERATURE ANALYSIS

- **CELL NUCLEUS SEGMENTATION OF SKIN TUMOR USING IMAGE PROCESSING**

  Automation and evaluation of determination of tumor cell pictures have been read for these three decades in the field of medicinal imaging innovation. Numerous methods of picture preparing were proposed to take care of issues, for example, core division and arrangement. In any case, these investigations have basically centered around epithelial tumors. Division test was finished utilizing genuine tissue cell pictures of DF and DFSP to assess legitimacy of this framework. Shape qualities, for example, evaluation of comparability to circle were likewise figured from the sectioned areas to guarantee that a few contrasts among DF and DFSP is communicated in its circulation.

- **Border Detection on Digitized Skin Tumor Images**

  A radial search technique is exhibited for recognizing skin tumor outskirts in clinical dermatology pictures. Initially, it incorporates two rounds of outspread pursuit dependent on a similar tumor focus. The first-round pursuit is free, and the second-round hunt is information based following. At that point a rescan with another middle is utilized to take care of the vulnerable side issue. The calculation is tried on model pictures with great execution, and on 300 genuine clinical pictures with an agreeable outcome.

- **Automatic Color Segmentation of Images with Application to Detection of Variegated Coloring in Skin Tumors**

  This paper depicts a PC vision framework to fill in as the front-part of the arrangement master framework that will mechanize visual element ID for skin tumor assessment. The general methodology is to make distinctive programming modules that will recognize the nearness or nonattendance of basic highlights. Picture investigation with computerized reasoning (AI) procedures, for example, the utilization of heuristics consolidated into picture preparing calculations, is the essential methodology.

- **Neural Network Diagnosis of Malignant Melanoma From Color Images**

In this paper, a novel neural network approach for the computerized partition of melanoma from three benign classifications of tumors which display melanoma-like qualities. Our methodology utilizes discriminant highlights, in light of tumor shape and relative tumor shading, that are provided to a fake neural network for grouping of tumor pictures as malignant or benign. With this methodology, for sensibly adjusted trainindtesting sets, we can acquire above 80% right characterization of the malignant and benign tumors on genuine skin tumor pictures.

- ## Identification of Variegated Coloring in Skin Tumor

Presently, variegated shading is the term frequently used to depict the shifted tones present in malignant melanoma, regularly including tan, dark colored, and red, and here and there shades of pink and blue. Variegated shading is accepted to be one of the most prescient highlights for malignant melanoma, yet it stays unclear with the exception of by model. In this article, we portray the utilization of neural networks for programmed distinguishing proof of variegated shading.

- ## Dermoscopic Image Segmentation via Multistage Fully Convolutional Networks

In this paper, proposition is to use completely convolutional networks (FCNs) to naturally portion the skin injuries. FCNs are a neural network design that accomplishes object location by progressively joining low-level appearance data with abnormal state semantic data. We address the issue of FCN delivering coarse division limits for testing skin sores (e.g., those with fluffy limits as well as low distinction in the surfaces between the frontal area and the foundation) through a multistage division approach in which numerous FCNs learn corresponding visual attributes of various skin sores; beginning period FCNs learn coarse appearance and limitation data while late-organize FCNs get familiar with the inconspicuous qualities of the injury limits.

- ## Detection of Skin Cancer by Classification of Raman Spectra

Skin lesion classification based on in vitro Raman spectroscopy is approached using a nonlinear neural network classifier. The classification framework is probabilistic and highly automated. The framework includes a feature extraction for Raman spectra and a fully adaptive and robust feedforward neural network classifier. Small distinctive bands in the spectrum, corresponding to specific lipids and proteins, are shown to hold the discriminating information which the network uses to diagnose skin lesions.

- **Automatic Skin Lesion Segmentation Using Deep Fully Convolutional Networks With Jaccard Distance**

  Proposition is a set of strategies to ensure effective and efficient learning with limited training data. Furthermore, we design a novel loss function based on Jaccard distance to eliminate the need of sample re-weighting, a typical procedure when using cross entropy as the loss function for image segmentation due to the strong imbalance between the number of foreground and background pixels. The method is general enough and only needs minimum pre- and post-processing, which allows its adoption in a variety of medical image segmentation tasks.

- **Dermoscopy Image Analysis: Overview and Future Directions**

  With the release of a large public dataset by the International Skin Imaging Collaboration in 2016, development of opensource software for convolutional neural networks, and the availability of inexpensive graphics processing units, dermoscopy image analysis has recently become a very active research field. In this paper, we present a brief overview of this exciting subfield of medical image analysis, primarily focusing on three aspects of it, namely, segmentation, feature extraction, and classification.

- **Detection of Skin Tumor Boundaries in Color Images**

  The method makes use of an adaptive color metric from the red, green, and blue (RGB) planes that contain information to discriminate the tumor from the background. Using this suitable coordinate transformation, the image is segmented. The tumor portion is then extracted from the segmented image and borders are drawn. Experimental results that verify the effectiveness of this approach are given.

- **SKAN: Skin Scanner – System for Skin Cancer Detection Using Adaptive Techniques**

  Its objective is to discern images of skin cancer, specifically melanoma, from others that show only common spots or other types of skin diseases, using image recognition. This work makes use of the ABCDE visual rule, which is often used by dermatologists for melanoma identification, to define which characteristics are analyzed by the software. It then applies various algorithms and techniques, including an ellipse-fitting algorithm, to extract and measure these characteristics and decide whether the spot is a melanoma or not.

- ## Detection and Analysis of Irregular Streaks in Dermoscopic Images of Skin Lesions

  This paper extends our previous algorithm to identify the absence or presence of streaks in a skin lesions, by further analyzing the appearance of detected streak lines, and performing a three-way classification for streaks, Absent, Regular, and Irregular, in a pigmented skin lesion. In addition, the directional pattern of detected lines is analyzed to extract their orientation features in order to detect the underlying pattern. The method uses a graphical representation to model the geometric pattern of valid streaks and the distribution and coverage of the structure.

- ## Overview of Advanced Computer Vision Systems for Skin Lesions Characterization

  We describe how to extract these features through digital image processing methods, i.e., segmentation, border detection, and color and texture processing, and we present the most prominent techniques for skin lesion classification. The paper reports the statistics and the results of the most important implementations that exist in the literature, while it compares the performance of several classifiers on the specific skin lesion diagnostic problem and discusses the corresponding findings.

- ## Accurate Segmentation of Dermoscopic Images by Image Thresholding Based on Type-2 Fuzzy Logic

  A novel thresholding-based segmentation approach for accurate segmentation of pigmented skin lesion images regarding malignant melanoma diagnosis has been proposed. The presented approach utilizes type-2 fuzzy logic techniques for automatic threshold determination. The method is applied on various clinically obtained lesion images, and the results are compared with those obtained with two other popular methods from the literature. It is observed that the presented method exhibits superior performance over competing methods and is very successful at handling the uncertainty encountered in determining the border between the lesion and the skin.

- ## Compression of Skin Tumor Images

  The need for high-performance compression algorithms to reduce storage and transmission costs is evident. The compression techniques described herein are likely to be effective for i! far wider range of images than the skin tumor images employed in this research.

- **Systematic Design of a Cross-Polarized Dermoscope for Visual Inspection and Digital Imaging**

  Adermoscope is a demonstrative gadget that can picture the skin in situ and is utilized for early analysis of melanoma and pigmented skin injuries. In this paper, we portray the plan and development of a cross-enraptured dermoscope including the light assessment, imaging structure, and the mechanical arrangement. By utilizing the cross-polarization dermoscope, specular reflection from the shallow layer of the skin is to a great extent dispensed with. Subsequently, more profound layers of the skin, for example, the internal colors and the slender veins, can be envisioned.

- **Development of a System Classification of Images Dermoscopic for Mobile Devices**

  A few endeavors have been occupied with the improvement of PC frameworks that guide in the conclusion of skin injuries and specifically melanoma. In the present paper shows the improvement of a dermoscopic picture characterization framework for cell phones. The framework breaks down the skin sores from the edge attributes and shade of the ABCD rule, and orders the sore utilizing a MLP network prepared with the backpropagation calculation. Whose objective is to give an instrument equipped for directing the assessment of dermoscopy in any area and enable it to be completed by various wellbeing experts. As indicated by the outcomes, the framework accomplished a degree of 66% affectability and 93% explicitness.

- **Automated Melanoma Recognition in Dermoscopy Images via Very Deep Residual Networks**

  They apply the dermoscopy figuring out how to adapt to the debasement and overfitting issues when a network goes further. This method can guarantee that our networks profit by the presentation additions accomplished by expanding network profundity. At that point, we develop a completely convolutional remaining network (FCRN) for precise skin injury division, and further improve its capacity by fusing a multi-scale logical data combination plot. At long last, we consistently incorporate the proposed FCRN (for division) and other profound remaining networks (for characterization) to shape a two-organize structure.

- **A New Algorithm for Border Description of Polarized Light Surface Microscopic Images of Pigmented Skin Lesions**

The point of this examination was to give numerical descriptors to the outskirt of pigmented skin sore pictures and to survey their viability for differentiation among various sore gatherings. New descriptors, for example, injury incline and sore slant consistency are presented and scientifically characterized. Another calculation dependent on the Catmull–Rom spline strategy and the calculation of the dark level inclination of focuses separated by insertion of typical bearing on spline focuses was utilized. The adequacy of these new descriptors was tried on an informational collection of 510 pigmented skin sores, created by 85 melanomas and 425 nevi, by utilizing factual strategies for segregation between the two populaces.

- **Anisotropic Mean Shift Based Fuzzy C-Means Segmentation of Dermoscopy Images**

The proposed division technique consolidates a mean field term inside the standard fluffy c-implies target work. Since mean move can rapidly and dependably discover bunch focuses, the whole system is able to do successfully distinguishing districts inside a picture. Exploratory outcomes on an enormous dataset of assorted dermoscopy pictures show that the exhibited strategy precisely and productively identifies the outskirts of skin sores.

- **Skin Lesion Classification Using Convolutional Neural Network With Novel Regularizer**

One of the most well-known sorts of human malignancies is skin disease, which is mainly analyzed outwardly, starting with a clinical screening pursued by dermoscopic investigation, histopathological appraisal, and a biopsy. Because of the fine-grained contrasts in the presence of skin injuries, computerized arrangement is very testing through pictures. To achieve exceptionally isolated and conceivably broad errands against the finely grained item ordered, profound convolutional neural networks (CNNs) are utilized. In this paper, we propose another forecast model that arranges skin sores into benign or malignant injuries dependent on a novel regularizer strategy.

- **DermaKNet: Incorporating the Knowledge of Dermatologists to Convolutional Neural Networks for Skin Lesion Diagnosis**

This paper presents DermaKNet, a CAD framework dependent on CNNs that joins explicit subsystems demonstrating properties of skin sores that are of extraordinary enthusiasm to dermatologists expecting to improve the interpretability of its determination. Our outcomes

demonstrate that the consolidation of these subsystems improves the exhibition, yet in addition upgrades the conclusion by giving progressively interpretable yields.

Module description

Processes involved in Image Processing:

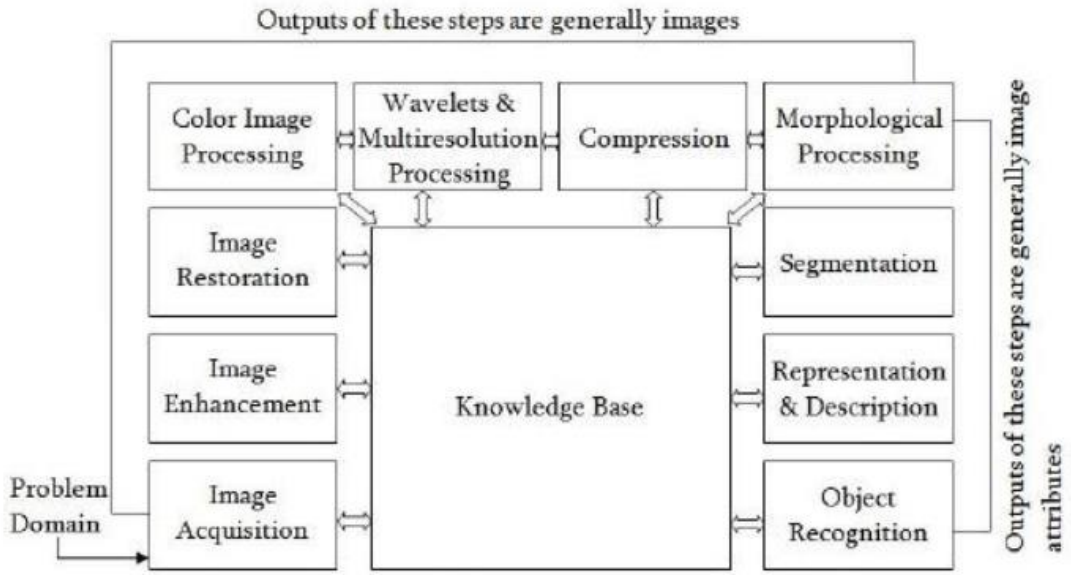

1. Image Acquisition

This is the initial step or procedure of the major strides of computerized picture handling. Picture procurement could be as straightforward as being given a picture that is as of now in advanced structure. By and large, the picture procurement arrange includes pre-preparing, for example, scaling and so forth.

2. Image Enhancement

Picture upgrade is among the least difficult and most engaging territories of advanced picture preparing. Essentially, the thought behind improvement methods is to bring out detail that is clouded, or just to feature certain highlights of enthusiasm for a picture. For example, changing splendor and complexity and so forth.

3. Image Restoration

Image restoration is an area that also deals with improving the appearance of an image. However, unlike enhancement, which is subjective, image restoration is objective, in the sense that restoration techniques tend to be based on mathematical or probabilistic models of image degradation.

We are applying various filters such median , average, gaussian etc.

4. Segmentation

Segmentation procedures partition an image into its constituent parts or objects. In general, autonomous segmentation is one of the most difficult tasks in digital image processing. A rugged segmentation procedure brings the process a long way toward successful solution of imaging problems that require objects to be identified individually.

5. Representation and Description

Representation and description almost always follow the output of a segmentation stage, which usually is raw pixel data, constituting either the boundary of a region or all the points in the region itself. Choosing a representation is only part of the solution for transforming raw data into a form suitable for subsequent computer processing. Description deals with extracting attributes that result in some quantitative information of interest or are basic for differentiating one class of objects from another.

6. Object classification

Classification of benign and malignant tumor images.

LIMITATIONS

The space of uses that can be actualized with this basic procedure is almost unending. But then, a lot more applications are totally distant for current profound learning strategies—even given huge measures of human-clarified information.

State, for example, that you could amass a dataset of several thousands—even millions—of English language depictions of the highlights of a product item, as composed by an item chief, just as the relating source code created by a group of specialists to meet these necessities. Indeed, even with this information, you couldn't prepare a profound learning model to just peruse an item portrayal and create the proper codebase.

That is only one model among many. All in all, anything that requires thinking—like programming, or applying the logical strategy—long haul arranging, and algorithmic-like information control, is distant for profound learning models, regardless of how much information you toss at them. In any event, learning an arranging calculation with a profound neural system is massively troublesome.

This is on the grounds that a profound learning model is "only" a chain of basic, ceaseless geometric changes mapping one vector space into another. Everything it can do is map one information complex X into another complex Y, accepting the presence of a learnable nonstop change from X to Y, and the accessibility of a thick testing of X:Y to use as preparing information.

So despite the fact that a profound learning model can be deciphered as a sort of program, conversely most projects can't be communicated as profound learning models—for most assignments, either there exists no comparing for all intents and purposes estimated profound neural system that fathoms the undertaking, or regardless of whether there exists one, it may not be learnable, for example the comparing geometric change might be very unpredictable, or there may not be suitable information accessible to learn it.

Scaling up current profound learning systems by stacking more layers and utilizing all the more preparing information can just externally mitigate a portion of these issues. It won't take care of the more central issue that profound learning models are restricted in what they can speak to, and that the majority of the projects that one may wish to learn can't be communicated as a constant geometric transforming of an information complex.

Proposed Method

Convolutional Neural Network (CNN)

In neural networks, Convolutional neural network (ConvNets or CNNs) is one of the main categories to do images recognition, images classifications. Objects detections, recognition faces etc., are some of the areas where CNNs are widely used.

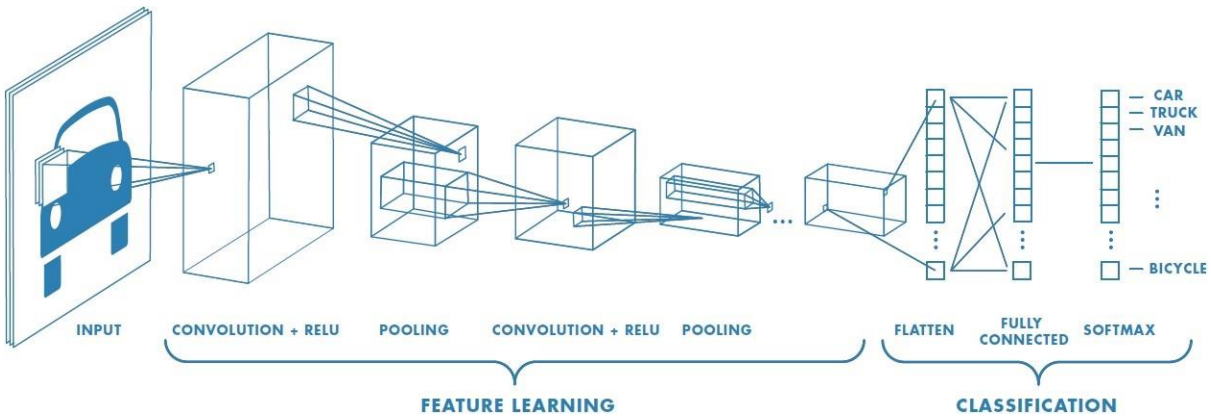

Figure 2 : Neural network with many convolutional layers

Convolution Layer

Convolution is the first layer to extract features from an input image. Convolution preserves the relationship between pixels by learning image features using small squares of input data. It is a mathematical operation that takes two inputs such as image matrix and a filter or kernal

- An image matrix (volume) of dimension **(h x w x d)**
- A filter **(f_h x f_w x d)**
- Outputs a volume dimension **(h - f_h + 1) x (w - f_w + 1) x 1**

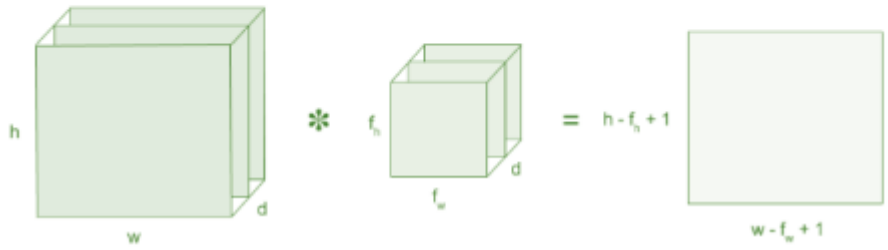

Figure 3: Image matrix multiplies kernel or filter matrix

Consider a 5 x 5 whose image pixel values are 0, 1 and filter matrix 3 x 3 as shown in below

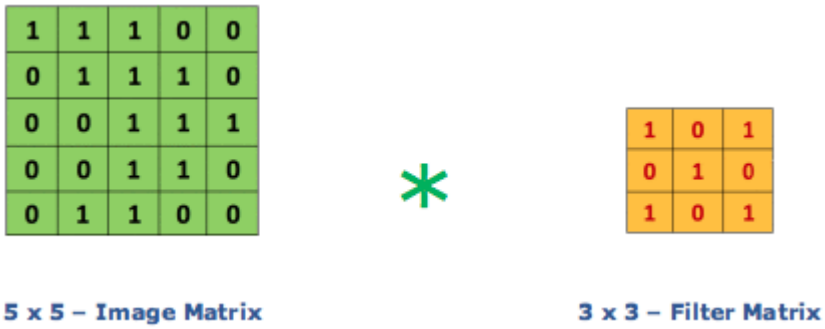

Figure 4: Image matrix multiplies kernel or filter matrix

Then the convolution of 5 x 5 image matrix multiplies with 3 x 3 filter matrix which is called **"Feature Map"** as output shown in below

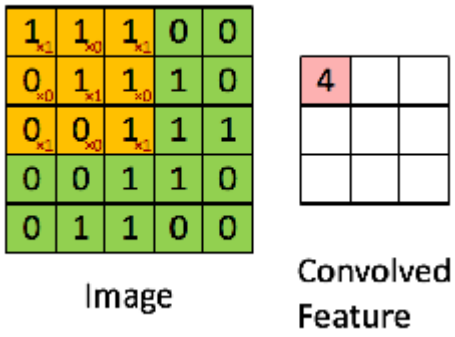

Figure 5: 3 x 3 Output matrix

Convolution of an image with different filters can perform operations such as edge detection, blur and sharpen by applying filters. The below example shows various convolution image after applying different types of filters (Kernels).

Strides

Stride is the number of pixels shifts over the input matrix. When the stride is 1 then we move the filters to 1 pixel at a time. When the stride is 2 then we move the filters to 2 pixels at a time and so on. The below figure shows convolution would work with a stride of 2.

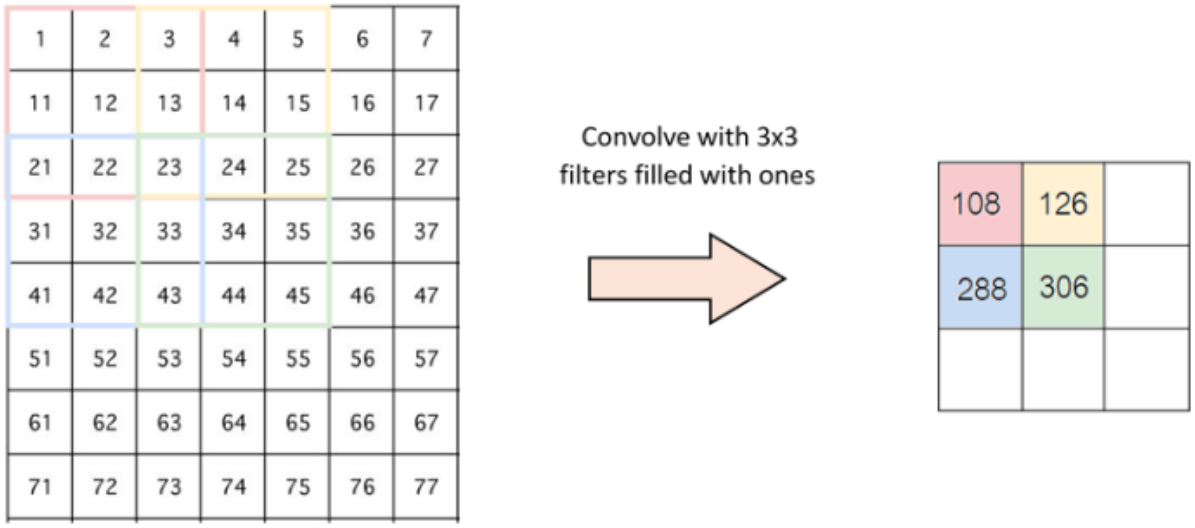

Figure 6 : Stride of 2 pixels

Padding

Sometimes filter does not fit perfectly fit the input image. We have two options:

- Pad the picture with zeros (zero-padding) so that it fits
- Drop the part of the image where the filter did not fit. This is called valid padding which keeps only valid part of the image.

Non Linearity (ReLU)

ReLU stands for Rectified Linear Unit for a non-linear operation. The output is $f(x) = max(0,x)$.

Why ReLU is important : ReLU's purpose is to introduce non-linearity in our ConvNet. Since, the real world data would want our ConvNet to learn would be non-negative linear values.

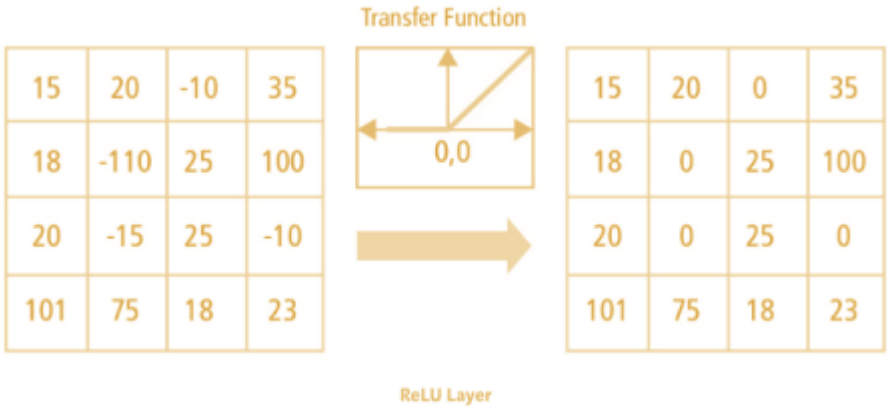

Figure 7 : ReLU operation

There are other non linear functions such as tanh or sigmoid can also be used instead of ReLU. Most of the data scientists uses ReLU since performance wise ReLU is better than other two.

Pooling Layer

Pooling layers section would reduce the number of parameters when the images are too large. Spatial pooling also called subsampling or downsampling which reduces the dimensionality of each map but retains the important information. Spatial pooling can be of different types:

- Max Pooling

- Average Pooling
- Sum Pooling

Max pooling take the largest element from the rectified feature map. Taking the largest element could also take the average pooling. Sum of all elements in the feature map call as sum pooling.

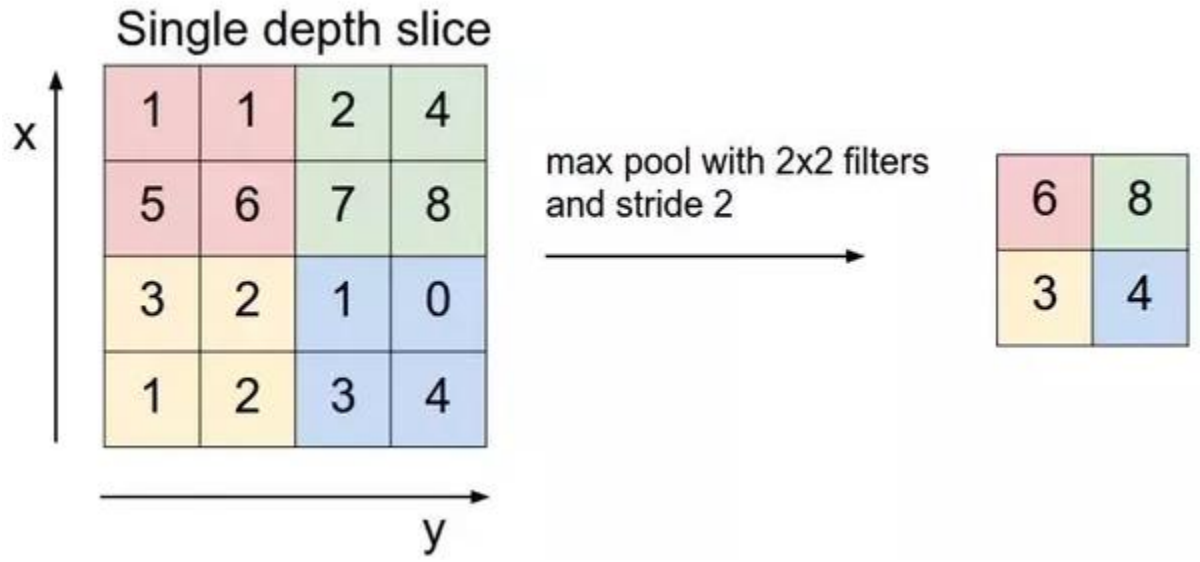

Figure 8 : Max Pooling

Fully Connected Layer

The layer we call as FC layer, we flattened our matrix into vector and feed it into a fully connected layer like neural network.

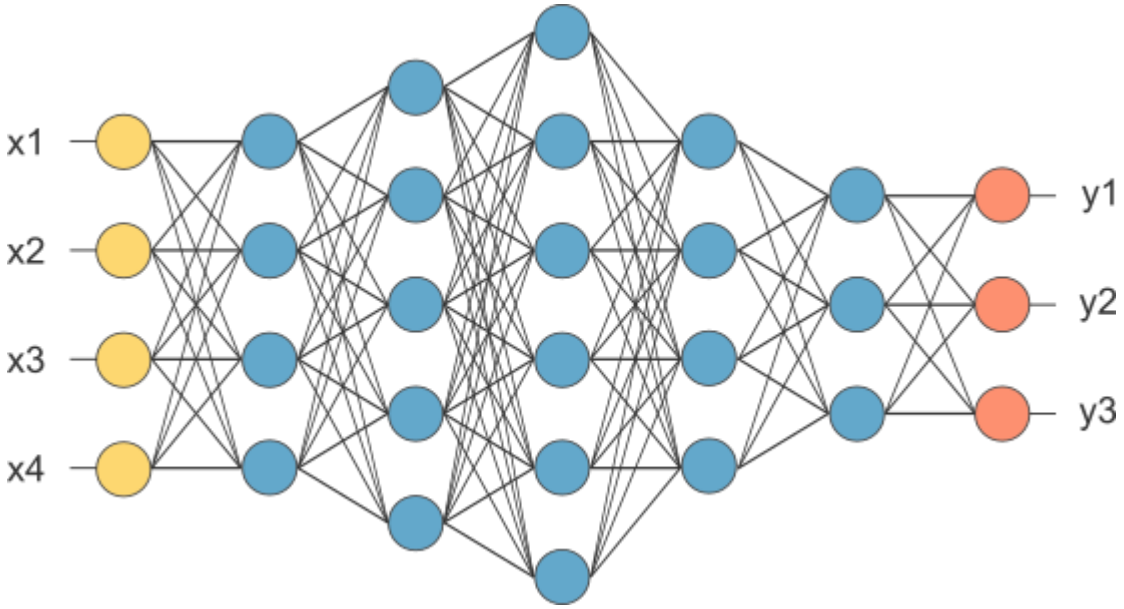

Figure 9 : After pooling layer, flattened as FC layer

In the above diagram, feature map matrix will be converted as vector (x1, x2, x3, …). With the fully connected layers, we combined these features together to create a model. Finally, we have an activation function such as softmax or sigmoid to classify the outputs as cat, dog, car, truck etc.,

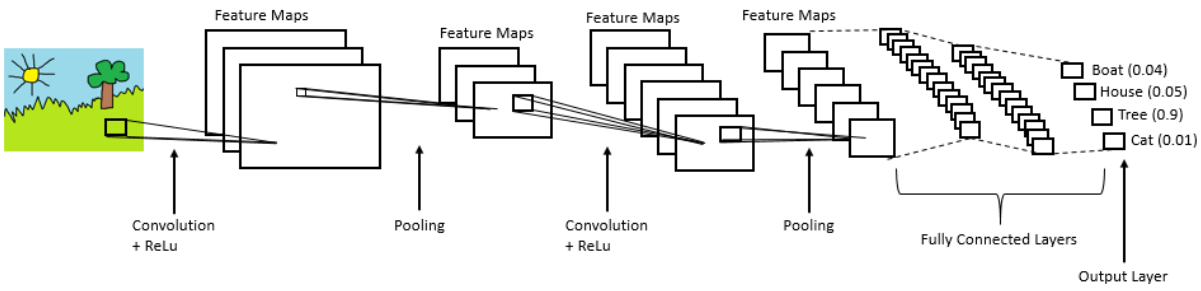

Architecture

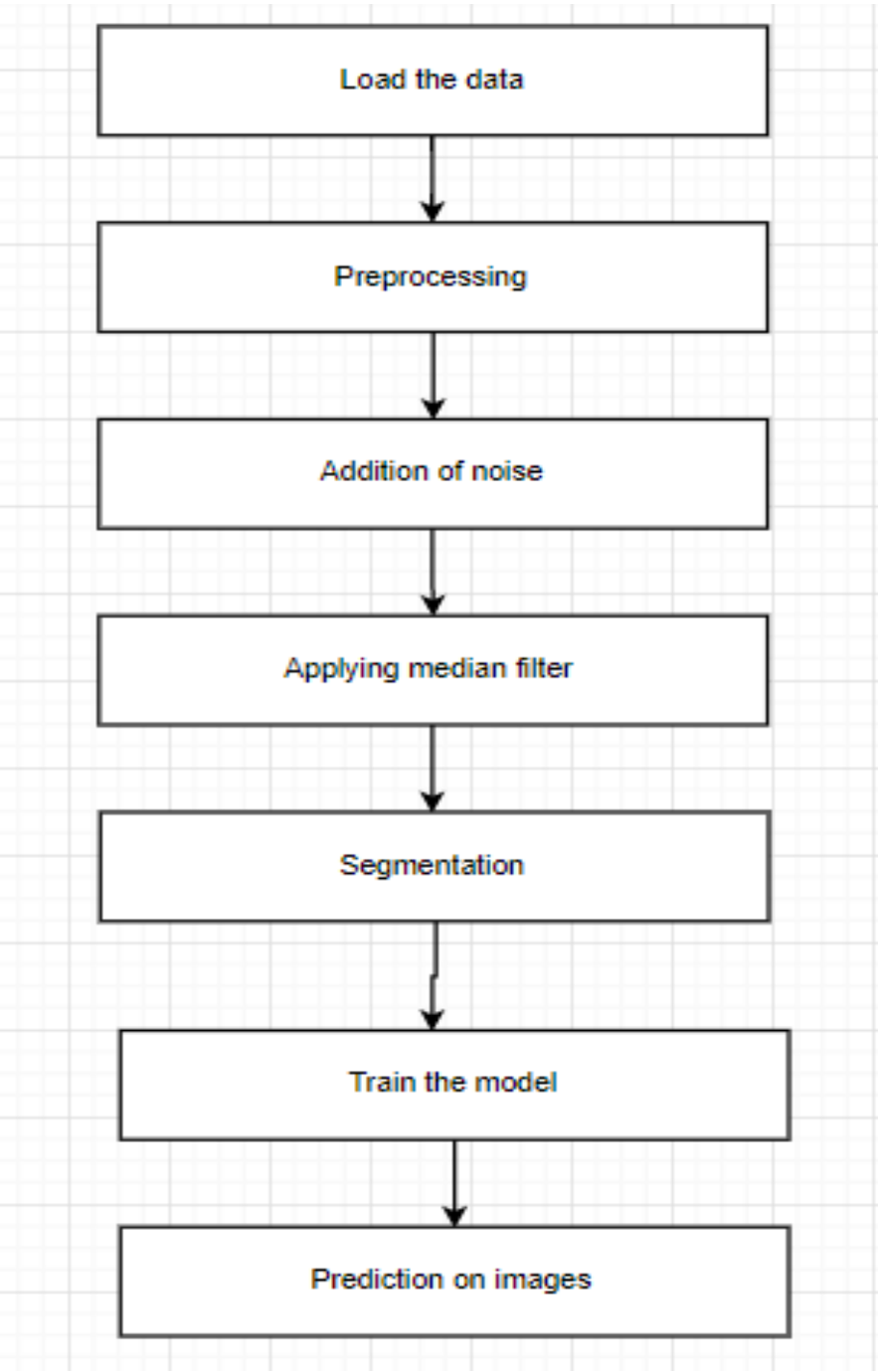

IMPLEMENTATION

1. Acquisition of data

```
from matplotlib import pyplot as plt
img = cv2.imread("./train/original/malignant/1000.jpg")
im = cv2.imread("./train/original/malignant/1000.jpg")
im = cv2.cvtColor(im, cv2.COLOR_BGR2RGB)
```

```
[64]: <matplotlib.image.AxesImage at 0x2630e3a00b8>
```

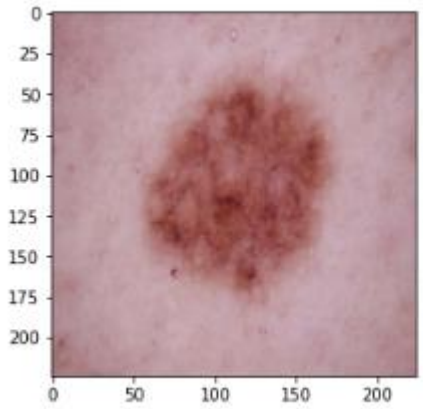

2. Addition of noise

```
img_noise = cv2.imread("./train/noise/malignant/1000.jpg")
img_noise = cv2.cvtColor(img_noise, cv2.COLOR_BGR2RGB)
plt.imshow(img_noise)
```

```
<matplotlib.image.AxesImage at 0x2630dd20470>
```

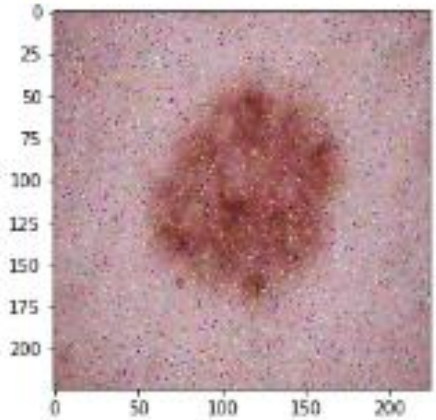

3. Image Restoration by applying filters

Gaussian blur

```
blur = cv2.GaussianBlur( im,(5,5),0)
```

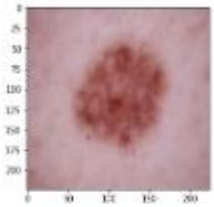

Median Filtering

```
img_median = cv2.medianBlur(img_noise,5)
```

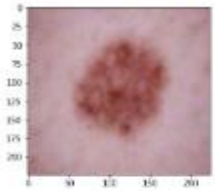

Bilateral filter

```
blur= cv2.bilateralFilter(im,9,75,75)
```

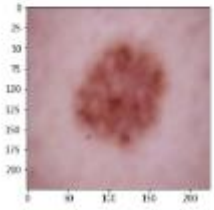

Average-filter

```
kernel = np.ones((5,5),np.float32)/25
dst = cv2.filter2D(im,-1,kernel)
```

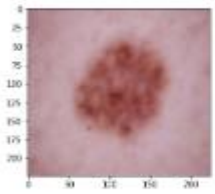

Laplacian

```
laplacian = cv2.Laplacian(blur,cv2.CV_64F)
plt.imshow(laplacian);
```

```
Clipping input data to the valid range for imshow with
```

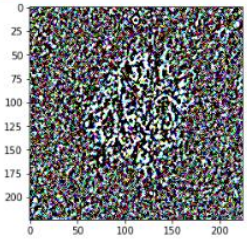

Negative image

```
imagem = cv2.bitwise_not(im);
plt.imshow(imagem);
```

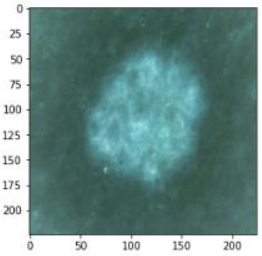

Hybrid Median Filter

```
n=5
img = np.zeros(img_noise.shape,dtype=np.int16)
# Derive indices for the two patterns representing X and +
indicesC = [0,4,6,8,12,16,18,20,24]
indicesP = [2,7,10,11,12,13,14,17,22]

v =int( (n-1) / 2)


# Process the image (ignoring the outer two layers of the image boundary
for i in range(2,img_noise.shape[0]-2):
    for j in range(2,img_noise.shape[1]-2):
            # Extract the neighbourhood area
        block = img_noise[i-v:i+v+1, j-v:j+v+1]

        # Reshape the neighborhood into a vector by flattening the 2D block
        wB = block.flatten()

            # Extract pixel values using indices
        wBc = np.take(wB,indicesC)
        wBp = np.take(wB,indicesP)

            # Calculate the median values
        wBcMed = int(np.median(wBc))

        wBpMed = int(np.median(wBp))

            # Calculate the hybrid median of the original pixel, and the two
            # medians extracted above
        lis=[wBcMed,wBpMed]


        xmed = np.median(lis)

            # Assign the values
        if (xmed > 0):
            img[i][j] = int(xmed)
        else:
            img[i][j] = im[i][j]

plt.imshow(img)
```

```
<matplotlib.image.AxesImage at 0x2630cc57f28>
```

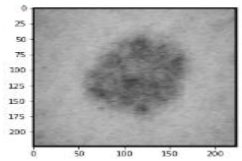

4. Segmentation of images

```
[52]: markers = cv2.watershed(img_median,markers)
      img_median[markers == -1] = [255,0,0]
      plt.imshow(img_median)
```

```
[52]: <matplotlib.image.AxesImage at 0x2630dd8dac8>
```

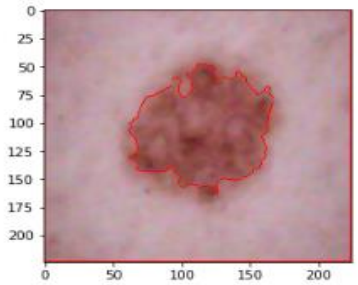


```
[53]: img_median[markers == 1] = 0
      plt.imshow(img_median)
```

```
[53]: <matplotlib.image.AxesImage at 0x2630ddeb518>
```

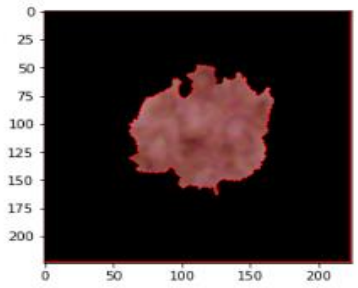

Extracting GLCM features

- Correlation
- Homogeneity
- Energy
- Contrast

```
img = cv2.cvtColor(img, cv2.COLOR_RGB2GRAY)
from xtract_features.glcms import *
feats = glcm(img)

# energy
energy = feats.energy()
print("Energy")
print(energy)
# correlation
corr = feats.correlation()
print("Correlation")
print(corr)
# contrast
cont = feats.contrast()
print("contrast")
print(cont)
# homogeneity
homogeneity = feats.homogeneity()
print("homogeneity")
print(homogeneity)
# all the features at once
_all = feats.glcm_all()
```

```
Energy
[0.03212519 0.03038586 0.03457699 0.03012517 0.0269988  0.03038586
 0.02884733 0.03012517 0.02515278 0.02640066 0.0269194  0.02594759]
Correlation
[0.99159036 0.98922846 0.99359272 0.98860316 0.98162389 0.98922846
 0.98613045 0.98860316 0.97282306 0.97858162 0.98009318 0.97674074]
contrast
[18.10169763 23.25401677 13.78287156 24.60393332 39.69729328 23.25401677
 29.92185489 24.60393332 58.9217841  46.54060141 43.07011555 50.54068257]
homogeneity
[0.29308294 0.26456691 0.33081454 0.26170785 0.21487723 0.26456691
 0.24416878 0.26170785 0.18584213 0.20467961 0.21167947 0.19688713]
```

Extracting Moments from an Image

```
from xtract_features.moments import *
img = cv2.cvtColor(im, cv2.COLOR_BGR2GRAY)
img = img.astype('uint8')
blur = cv2.GaussianBlur(img,(5,5),0)
ret3,th3 = cv2.threshold(blur,0,255,cv2.THRESH_BINARY | cv2.THRESH_OTSU)
image = np.invert(th3)
_moments = moments(image).get_moments()
print(_moments)
_hu_moments = moments(image).get_HuMoments()
print()
print("_hu_moments :")
print(_hu_moments)
```

```
[2586465.0, 292979700.0, 282005775.0, 35701014900.0, 31202688675.0, 33678899835.0, 4550315037480.0, 3762991195845.0, 3599437922415.0, 433907737225.0, 2513979849.4232445, -741284028.1943207, 2931429007.6929893, -63226131365.37988, 97965018.091
65414864.34717, 27786066345.959473, 0.0003757920859074, -0.0001108080803077707, 0.0004381937402485399, -5.876653635181049e-06, 3.5689601092797175e-06, -5.006606908206793e-06, 2.582620259584238e-06]

_hu_moments :
[0.00081398664883928, 5.300758643755783e-08, 1.4960110608204782e-10, 1.5628730108985502e-10, 1.537788621966483e-20, 2.4644351946487657e-14, -1.8292412512518287e-20]
```

[85]:
```
# Extracting Region Properties
```

[86]:
```
from xtract_features.region_props import *
_rp = region_props(img)
# maximum area region
max_area = _rp.max_area()
print (" Max Area :")
print(max_area)
# plot regions
_rp.plot_image()
# plot black and white
_rp.plot_show_bw()
# plot with lables
_rp.plot_image_with_label()
# mean of areas of all the regions
_rp.mean_area()
# eccentricity of the highest area region
_rp.eccentricity()
```

```
 Max Area :
13
```

[86]:
```
0.4175631381707138
```

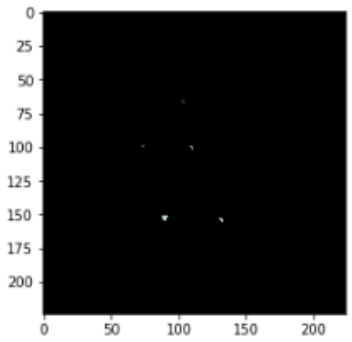

]:
```
# Entropy
```

]:
```
from xtract_features.extract import s_entropy, entropy_simple
# shannon's entropy
s_entr = s_entropy(img)
# simple entropy
entr_simp = entropy_simple(img)
print("shannon's entropy")
print(s_entr)
print("simple entropy")
print(entr_simp)
```

```
shannon's entropy
6.254261104713153
simple entropy
4.335123451217649
```

5. Applying Convolutional nueral net

Creating the Model - CNN

```
from keras.models import Sequential
from keras.layers import Activation, Dropout, Flatten, Dense, Conv2D, MaxPooling2D
```

```
model = Sequential()

model.add(Conv2D(filters=32, kernel_size=(3,3),input_shape=image_shape, activation='relu',))
model.add(MaxPooling2D(pool_size=(2, 2)))
model.add(Dropout(0.25))
model.add(Conv2D(filters=64, kernel_size=(3,3), activation='relu'))
model.add(MaxPooling2D(pool_size=(2, 2)))
model.add(Conv2D(filters=64, kernel_size=(3,3), activation='relu'))
model.add(MaxPooling2D(pool_size=(2, 2)))
model.add(Dropout(0.25))
model.add(Conv2D(filters=128, kernel_size=(3,3), activation='relu'))
model.add(MaxPooling2D(pool_size=(2, 2)))
model.add(Conv2D(filters=128, kernel_size=(3,3), activation='relu',))
model.add(MaxPooling2D(pool_size=(2, 2)))
model.add(Conv2D(filters=128, kernel_size=(3,3), activation='relu',))
model.add(MaxPooling2D(pool_size=(2, 2)))
model.add(Flatten())


model.add(Dense(256))
model.add(Activation('relu'))

# Dropouts help reduce overfitting by randomly turning neurons off during training.
# Here we say randomly turn off 50% of neurons.
model.add(Dropout(0.5))

# Last layer only one dense, remember its binary, 0=Benign , 1=Malignant
model.add(Dense(1))
model.add(Activation('sigmoid'))

#loss fn  -  binar_crossentropy bcs 0 or 1 prediction
model.compile(loss='binary_crossentropy',
              optimizer='adam',
              metrics=['accuracy'])
```

```
model.summary
```

Training the Model

```
batch_size = 16

train_image_gen = image_gen.flow_from_directory('../skin-cancer-malignant-vs-benign/train/original',
                                                target_size=image_shape[:2],
                                                batch_size=batch_size,
                                                class_mode='binary')
```

```
Found 2643 images belonging to 2 classes.
```

```
test_image_gen = image_gen.flow_from_directory('../skin-cancer-malignant-vs-benign/test/original',
                                                target_size=image_shape[:2],
                                                batch_size=batch_size,
                                                class_mode='binary')
```

```
Found 660 images belonging to 2 classes.
```

```
train_image_gen.class_indices
```

```
{'benign': 0, 'malignant': 1}
```

```
#the number of samples processed for each epoch is batch_size * steps_per_epochs
results = model.fit_generator(train_image_gen,epochs=50,
                              steps_per_epoch=50,
                              validation_data=test_image_gen,
                             validation_steps=12,
                             )
```

```
50/50 [==============================] - 13s 261ms/step - loss: 0.3453 - acc: 0.8350 - val_loss: 0.2706 - val_acc: 0.8958
Epoch 88/100
50/50 [==============================] - 14s 287ms/step - loss: 0.3123 - acc: 0.8625 - val_loss: 0.3362 - val_acc: 0.8667
Epoch 89/100
50/50 [==============================] - 12s 234ms/step - loss: 0.2993 - acc: 0.8622 - val_loss: 0.4036 - val_acc: 0.8125
Epoch 90/100
50/50 [==============================] - 13s 260ms/step - loss: 0.3255 - acc: 0.8475 - val_loss: 0.3847 - val_acc: 0.8177
Epoch 91/100
50/50 [==============================] - 13s 253ms/step - loss: 0.3077 - acc: 0.8685 - val_loss: 0.2684 - val_acc: 0.8556
Epoch 92/100
50/50 [==============================] - 13s 266ms/step - loss: 0.3143 - acc: 0.8600 - val_loss: 0.3226 - val_acc: 0.8542
Epoch 93/100
50/50 [==============================] - 13s 261ms/step - loss: 0.2942 - acc: 0.8588 - val_loss: 0.3909 - val_acc: 0.8333
Epoch 94/100
50/50 [==============================] - 13s 259ms/step - loss: 0.3253 - acc: 0.8500 - val_loss: 0.3890 - val_acc: 0.7917
Epoch 95/100
50/50 [==============================] - 14s 280ms/step - loss: 0.3039 - acc: 0.8557 - val_loss: 0.3246 - val_acc: 0.8611
Epoch 96/100
50/50 [==============================] - 12s 236ms/step - loss: 0.2833 - acc: 0.8538 - val_loss: 0.3629 - val_acc: 0.8542
Epoch 97/100
50/50 [==============================] - 13s 258ms/step - loss: 0.3092 - acc: 0.8550 - val_loss: 0.3567 - val_acc: 0.8333
Epoch 98/100
50/50 [==============================] - 13s 257ms/step - loss: 0.2896 - acc: 0.8575 - val_loss: 0.3586 - val_acc: 0.8444
Epoch 99/100
50/50 [==============================] - 13s 265ms/step - loss: 0.3033 - acc: 0.8689 - val_loss: 0.3880 - val_acc: 0.8177
Epoch 100/100
50/50 [==============================] - 13s 261ms/step - loss: 0.3152 - acc: 0.8560 - val_loss: 0.3550 - val_acc: 0.8229
```

```python
import numpy as np
print(np.mean(results.history['acc']))
print(np.mean(results.history['val_acc']))
print(np.mean(results.history['loss']))
print(np.mean(results.history['val_loss']))
```

```
0.8101276976732715
0.7994236111111112
0.38984467822545105
0.40452211956638434
```

Evaluating the Model

```
[ ]  plt.plot(results.history['acc'])
     plt.plot(results.history['val_acc'])
     plt.title('model accuracy')
     plt.ylabel('accuracy')
     plt.xlabel('epoch')
     plt.show()
```

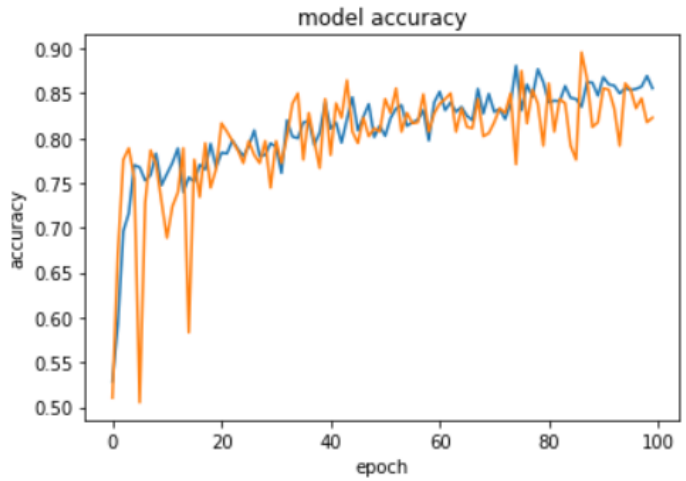


```
[ ]  plt.plot(results.history['loss'])
     plt.plot(results.history['val_loss'])
     plt.title('model loss')
     plt.ylabel('loss')
     plt.xlabel('epoch')
     plt.legend(['train', 'test'], loc='upper left')
     plt.show()
```

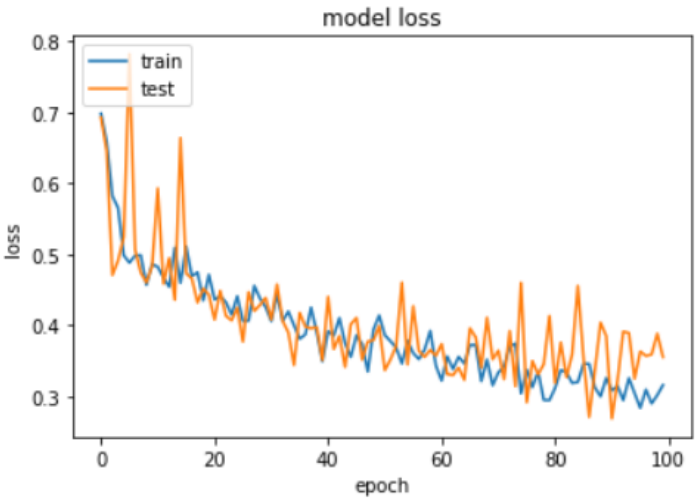

Predicting new images

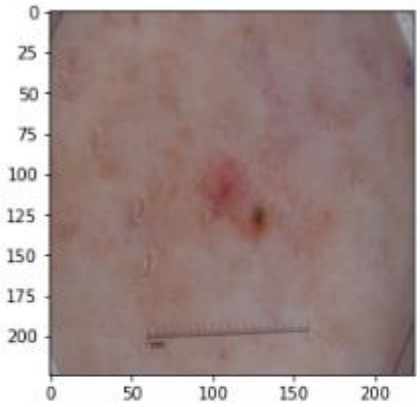


```
prediction_prob = model.predict(img)
```

```
# Output prediction
if(prediction_prob>0.5):
    print("Its a malignant tumour")
else:
    print("Its a benign tumour")
```

```
Its a malignant tumour
```

Comparative analysis

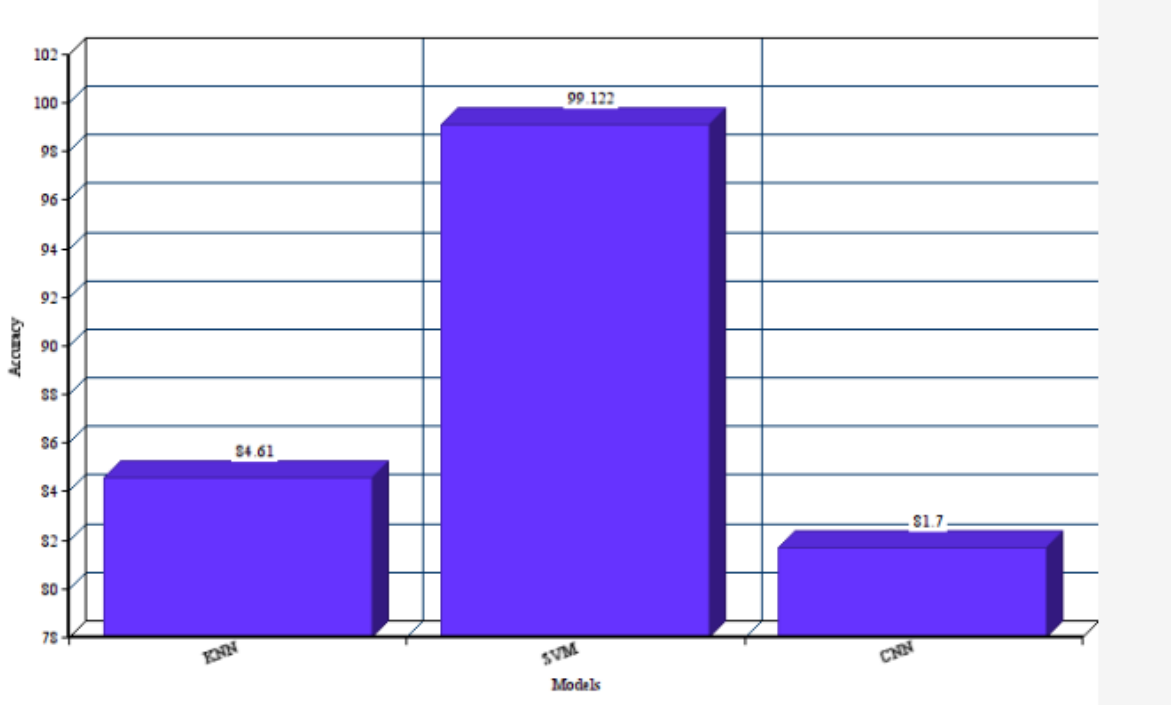

Conclusion

Noisy data was applied with filtered to get clean data which further segmented. Proper classification of skin cancer images, for accurate identification of type of tumor, is of great importance. CNN technology can learn and automatically determine what features are important for classification from the training image set.We have thus proposed a model which can classify between malignant
and benign tumor with an accuracy of about 81.09%.

REFERENCES

1.Z. Zhang, W. V. Stoecker and R. H. Moss, "Border detection on digitized skin tumor images," in IEEE Transactions on Medical Imaging, vol. 19, no. 11, pp. 1128-1143, Nov. 2010.

doi: 10.1109/42.896789

2.T. Tanaka, T. Joke and T. Oka, "Cell nucleus segmentation of skin tumor using image processing," 2001 Conference Proceedings of the 23rd Annual International Conference of the IEEE Engineering in Medicine and Biology Society, Istanbul, Turkey, 2011, pp. 2716-2719 vol.3.

3.S. E. Umbaugh, R. H. Moss and W. V. Stoecker, "Automatic color segmentation of images with application to detection of variegated coloring in skin tumors," in IEEE Engineering in Medicine and Biology Magazine, vol. 8, no. 4, pp. 43-50, Dec. 1999

4.A. Durg, W. V. Stoecker, J. P. Cookson, S. E. Umbaugh and R. H. Moss, "Identification of variegated coloring in skin tumors: neural network vs. rule-based induction methods," in IEEE Engineering in Medicine and Biology Magazine, vol. 12, no. 3, pp. 71-74, Sept. 2003.

5.F. Ercal, A. Chawla, W. V. Stoecker, Hsi-Chieh Lee and R. H. Moss, "Neural network diagnosis of malignant melanoma from color images," in IEEE Transactions on Biomedical Engineering, vol. 41, no. 9, pp. 837-845, Sept. 2004.

6. L. Bi, J. Kim, E. Ahn, A. Kumar, M. Fulham and D. Feng, "Dermoscopic Image Segmentation via Multistage Fully Convolutional Networks," in IEEE Transactions on Biomedical Engineering, vol. 64, no. 9, pp. 2065-2074, Sept. 2017

7. S. Sigurdsson, P. A. Philipsen, L. K. Hansen, J. Larsen, M. Gniadecka and H. C. Wulf, "Detection of skin cancer by classification of Raman spectra," in IEEE Transactions on Biomedical Engineering, vol. 51, no. 10, pp. 1784-1793, Oct. 2010.

8. Y. Yuan, M. Chao and Y. Lo, "Automatic Skin Lesion Segmentation Using Deep Fully Convolutional Networks With Jaccard Distance," in IEEE Transactions on Medical Imaging, vol. 36, no. 9, pp. 1876-1886, Sept. 2017.

9. Celebi, M. Emre & Codella, Noel & Halpern, Allan. (2019). Dermoscopy Image Analysis: Overview and Future Directions. IEEE Journal of Biomedical and Health Informatics. PP. 1-1. 10.1109/JBHI.2019.2895803.

10. F. Ercal, M. Moganti, W. V. Stoecker and R. H. Moss, "Detection of skin tumor boundaries in color images," in IEEE Transactions on Medical Imaging, vol. 12, no. 3, pp. 624-626, Sept. 2013.

11. H. de Souza Ganzeli, J. Godoy Bottesini, L. de Oliveira Paz and M. Figueiredo Salgado Ribeiro, "SKAN: Skin Scanner - System for Skin Cancer Detection Using Adaptive Techniques," in IEEE Latin America Transactions, vol. 9, no. 2, pp. 206-212, April 2011.

12. M. Sadeghi, T. K. Lee, D. McLean, H. Lui and M. S. Atkins, "Detection and Analysis of Irregular Streaks in Dermoscopic Images of Skin Lesions," in IEEE Transactions on Medical Imaging, vol. 32, no. 5, pp. 849-861, May 2013.

13. I. Maglogiannis and C. N. Doukas, "Overview of Advanced Computer Vision Systems for Skin Lesions Characterization," in IEEE Transactions on Information Technology in Biomedicine, vol. 13, no. 5, pp. 721-733, Sept. 2009.

14. M. E. YÜksel and M. Borlu, "Accurate Segmentation of Dermoscopic Images by Image Thresholding Based on Type-2 Fuzzy Logic," in IEEE Transactions on Fuzzy Systems, vol. 17, no. 4, pp. 976-982, Aug. 2011.

15. A. Kjoelen, S. E. Umbaugh and M. Zuke, "Compression of skin tumor images," in IEEE Engineering in Medicine and Biology Magazine, vol. 17, no. 3, pp. 73-80, May-June 1998.

16. H. Wang, X. Xu, X. Li, P. Xi and Q. Ren, "Systematic design of a cross-polarized dermoscope for visual inspection and digital imaging," in IEEE Instrumentation & Measurement Magazine, vol. 14, no. 6, pp. 26-31, December 2011.

17. F. E. S. Alencar, D. C. Lopes and F. M. Mendes Neto, "Development of a System Classification of Images Dermoscopic for Mobile Devices," in IEEE Latin America Transactions, vol. 14, no. 1, pp. 325-330, Jan. 2016.

18. C. Grana, G. Pellacani, R. Cucchiara and S. Seidenari, "A new algorithm for border description of polarized light surface microscopic images of pigmented skin lesions," in IEEE Transactions on Medical Imaging, vol. 22, no. 8, pp. 959-964, Aug. 2013.

19. L. Yu, H. Chen, Q. Dou, J. Qin and P. Heng, "Automated Melanoma Recognition in Dermoscopy Images via Very Deep Residual Networks," in IEEE Transactions on Medical Imaging, vol. 36, no. 4, pp. 994-1004, April 2017.

20. H. Zhou, G. Schaefer, A. H. Sadka and M. E. Celebi, "Anisotropic Mean Shift Based Fuzzy C-Means Segmentation of Dermoscopy Images," in IEEE Journal of Selected Topics in Signal Processing, vol. 3, no. 1, pp. 26-34, Feb. 2009.

21. M. A. Albahar, "Skin Lesion Classification Using Convolutional Neural Network With Novel Regularizer," in IEEE Access, vol. 7, pp. 38306-38313, 2019.

22. I. González-Díaz, "DermaKNet: Incorporating the Knowledge of Dermatologists to Convolutional Neural Networks for Skin Lesion Diagnosis," in IEEE Journal of Biomedical and Health Informatics, vol. 23, no. 2, pp. 547-559, March 2019.

23. A. Durg, W. V. Stoecker, J. P. Cookson, S. E. Umbaugh and R. H. Moss, "Identification of variegated coloring in skin tumors: neural network vs. rule-based induction methods," in IEEE Engineering in Medicine and Biology Magazine, vol. 12, no. 3, pp. 71-74, Sept. 2003.

24. F. Ercal, M. Moganti, W. V. Stoecker and R. H. Moss, "Detection of skin tumor boundaries in color images," in IEEE Transactions on Medical Imaging, vol. 12, no. 3, pp. 624-626, Sept. 2013.

Conference Papers:

25. F. E. S. Alencar, D. C. Lopes and F. M. Mendes Neto, "Development of a System Classification of Images Dermoscopic for Mobile Devices," in IEEE Latin America Transactions, vol. 14, no. 1, pp. 325-330, Jan. 2016

26. W. Safta and H. Frigui, "Multiple Instance Learning for Benign vs. Malignant Classification of Lung Nodules in CT Scans," 2018 IEEE International Symposium on Signal Processing and Information Technology (ISSPIT), Louisville, KY, USA, 2018, pp. 490-494.

27. D. R. Chittajallu et al., "Vectorized persistent homology representations for characterizing glandular architecture in histology images," 2018 IEEE 15th International Symposium on Biomedical Imaging (ISBI 2018), Washington, DC, 2018, pp. 232-235.

28. J. Y. Lo and C. E. Floyd, "Application of artificial neural networks for diagnosis of breast cancer," Proceedings of the 1999 Congress on Evolutionary Computation-CEC99 (Cat. No. 99TH8406), Washington, DC, USA, 1999, pp. 1755-1759 Vol. 3.

29. L. M. Bruce and R. Kalluri, "An analysis of the contribution of scale in mammographic mass classification," Proceedings of the 19th Annual International Conference of the IEEE Engineering in Medicine and Biology Society. 'Magnificent Milestones and Emerging Opportunities in Medical Engineering' (Cat. No.97CH36136), Chicago, IL, USA, 1997, pp. 1609-1612 vol.4.

30. S. Guan and M. Loew, "Breast Cancer Detection Using Transfer Learning in Convolutional Neural Networks," 2017 IEEE Applied Imagery Pattern Recognition Workshop (AIPR), Washington, DC, 2017, pp. 1-8.

BIBILIOGRAPHY

- https://www.kaggle.com/fanconic/skin-cancer-malignant-vs-benign
- https://machinelearningmastery.com/image-augmentation-deep-learningkeras /
- https://stats.stackexchange.com/questions/153531/what-is-batchsize-in-neural-network
- https://www.pyimagesearch.com/2018/12/31/keras-conv2d-and-convolutionallayers/targetText=filters,the%20convolutional%20layer%20will%20learn.
- https://www.pyimagesearch.com/2018/12/31/keras-conv2d-and-convolutionallayers/targetText=filters,the%20convolutional%20layer%20will%20learn
- https://towardsdatascience.com/a-comprehensive-guide-to-convolutionalneural-networks-the-eli5-way-3bd2b1164a53150
- https://medium.com/data-science-group-iitr/loss-functions-and-optimizationalgorithms-demystified-bb92daff331c
- https://towardsdatascience.com/beginners-guide-to-understandingconvolutional-neural-networks-ae9ed58bb17d
- https://towardsdatascience.com/beginners-guide-to-understandingconvolutional-neural-networks-ae9ed58bb17d